

Observation of transverse space charge effects in a mutli-beamlet electron bunch produced in a photo-emission electron source

M. Rihaoui*, W. Gai[†], P. Piot**, J. G. Power[†] and Z. Yusof[†]

**Department of Physics and Northern Illinois Center for Accelerator & Detector Development,
Northern Illinois University, IL 60115 DeKalb, USA*

[†]HEP Division, Argonne National Laboratory, Argonne, IL 60439, USA

***Department of Physics and Northern Illinois Center for Accelerator & Detector Development,
Northern Illinois University, IL 60115 DeKalb, USA*

and Accelerator Physics Center, Fermi National Accelerator Laboratory, Batavia IL 60510, USA

Abstract. A "multiple beamlet" experiment aimed at investigating the transverse space charge effect was recently conducted at the Argonne Wakefield Accelerator. The experiment generated a symmetric pattern of 5 beamlets on the photocathode of the RF gun with the drive laser. We explored the evolution of the thereby produced 5 MeV, space-charge dominated electron beamlets in the 2m drift following the RF photocathode gun for various external focusing. Two important effects were observed and benchmarked using the particle-in-cell beam dynamics code IMPACT-T. In this paper, we present our experimental observation and their benchmarking with Impact-T.

Keywords: photoinjector, space charge effects

PACS: 29.27.-a, 41.85.-p, 41.75.F

INTRODUCTION

Many accelerator applications call for the production of high charge (few nC) low transverse emittance (few μm) high peak current (several kA) electron bunches. Such applications range from accelerator-based light sources [1], high energy physics accelerator [2] to novel acceleration techniques, e.g., based on dielectric wakefield accelerators [3]. The dynamics of such very bright, space-charge-dominated, electron beams is intricate: it can develop transverse instabilities and is subject to, e.g., emittance diluting effects [4, 5]. Typically, high-brightness electron bunches are produced in a photoinjector: a high quantum efficiency photocathode, illuminated by a laser, is located on the back plate of a radio frequency (rf) resonant cavity and high charge bunch are photoemitted and rapidly accelerated to relativistic energies [6]. The electron bunch properties are set by the photocathode drive laser parameters. Several theoretical and experimental studies have addressed detrimental effects due to, e.g., laser transverse distribution non-uniformities. For instance Reference [7] experimentally explores the impact of transverse modulations on the root-mean-square (rms) transverse emittance. In most investigations, the beam is statistically characterized using its rms properties. Although this is a universal characterization relying on the concept of "equivalent beam" [8] important details of the beam evolutions might be missed. The pioneering work of Reiser and co-workers underlined the importance of studying the evolution of the beam's distribu-

tion and not only its rms properties [9, 10]. The experiment used a quincunx pattern to generate five beamlets transversely separated. In this Paper we present a similar experiment performed in a photoinjector using a ~ 5 MeV bunched electron beam. Shaping the transverse distribution of the photocathode drive-laser allowed the generation of a beam that consisted of several transversely separated beamlets. The evolution of the beamlets' transverse density provides information on transverse space charge effect which are validated against particle-in-cell (PIC) simulations.

EXPERIMENTAL SETUP AND RESULTS

Our experiment was performed at the Argonne Wakefield Accelerator (AWA) [11]; see Figure 1. The accelerator incorporates a photoemission source consisting of a 1+1/2

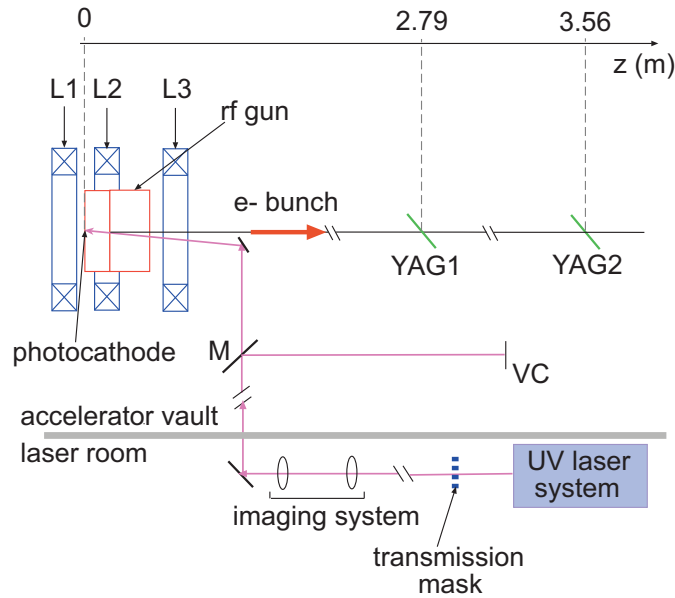


FIGURE 1. (Color) Overview of the AWA beam line. Here only the elements pertaining to our experiment are shown. The legend represent solenoidal magnetic lenses (L), optical mirror (M), virtual cathode (VC) and transverse density monitor (YAG1 and 2). The distance along the beamline is also shown.

cell rf cavity operating at $f = 1.3$ GHz, henceforth referred to as rf gun. An ultraviolet (uv) laser beam impinges a magnesium photocathode located on the back plate of the rf gun half cell. The thereby photoemitted electron bunch exits from the rf gun with a maximum kinetic energy of approximately 5 MeV and is allowed to drift for few meters with no external field. Two Yttrium Aluminum Garnet (YAG) screens located along the beamline are used to measure the beam's transverse density; see Figure 1. The operating conditions of the main subsystems of the photoinjector during the experiment reported herein are gathered in Table 1. The uv laser system consists of a Titanium Sapphire laser amplified with a regenerative amplifier. The infrared laser is frequency-tripled to $\lambda = 248$ nm and can be further amplified in a single-stage Krypton Fluoride excimer amplifier. The laser system is located ~ 20 m from the photocathode and the laser beam is transported via an optical imaging system. The transverse distribution on

the photocathode can be controlled by masks or irises placed in the object plane of the imaging system. This object plane is located in the laser room thereby allowing laser shaping without interrupting the accelerator operation. The laser beam temporal profile is a Gaussian distribution with rms duration of $\sigma_t \simeq 2$ ps. The rf gun is surrounded by three solenoidal magnetic lenses independently powered referred to as L1, L2 and L3 in Figure 1. During the experiment reported below only L3 was used. The transverse distribution of the uv laser on the photocathode can be directly inferred from an image of the laser beam on a "virtual photocathode." The virtual photocathode consists of a uv sensitive CCD camera, located outside of the vacuum chamber, and is a one-to-one optical image of the photocathode.

TABLE 1. Nominal accelerator settings during the experiment. The "Experiment" and "Model" columns respectively correspond to values inferred from the AWA control system and values obtained when matching the impact-T model to the single particle measurements.

Parameter (unit)	Experiment	Model
Laser rms pulse duration (ps)	1.915 ± 0.2	1.915
laser injection phase (deg)	50 ± 5	53
E-field on cathode (MV/m)	54 ± 3	51
L3 peak axial B-field (T)	$[0.30, 0.40] \pm 0.01$	[0.30, 0.40]
Charge - high charge (nC)	0.9 ± 0.1	0.9
Charge - low charge (nC)	0.015 ± 0.005	0.015
Kinetic Energy (MeV)	5.20 ± 0.10	5.28

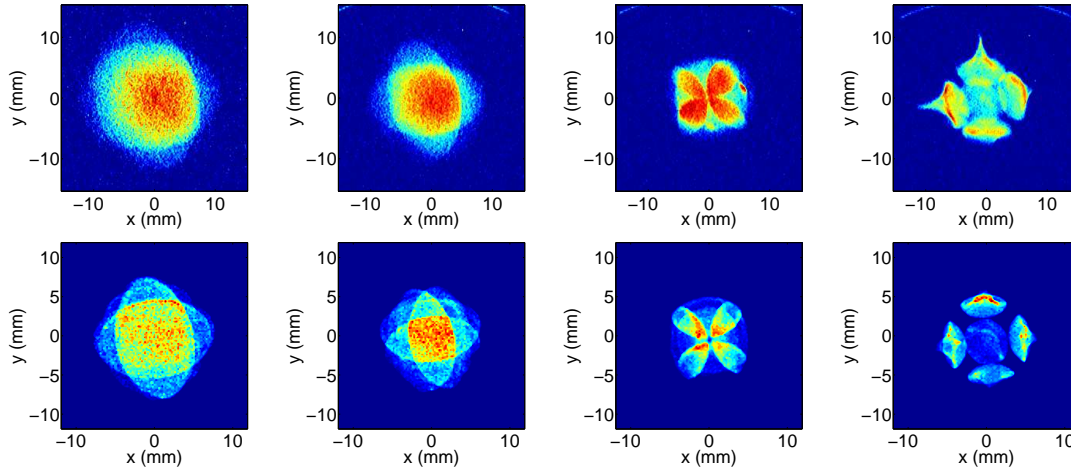


FIGURE 2. (Color) False color images of the measured (top row) and simulated (bottom row) electron beam transverse density distributions at YAG1 location. The four columns respectively correspond to different values of the magnetic field (from right column) $\hat{B} = 0.333, 0.339, 0.350, 0.359$ T.

We used a transmission mask located in the object plane of the photocathode image to tailor the laser transverse density. The mask consisted of a matrix of holes, bored in a 1 mm thick Aluminum plate, that could be obstructed thereby allowing an arbitrary number of beamlet patterns to be generated. The center-to-center hole separation is 2 mm and the holes diameter 1 mm. A first experiment consisted in generating a low charge electron beam consisting of six beams such to break the pattern symme-

try and be able to relate the beamlet observed on YAG1 screen to their locations on the photocathode. Due to low space charge effects, the beamlets do not interact and effectively behave as independent macroparticles. We performed a series of measurements to benchmark our numerical model of AWA in the quasi single-particle dynamics regime. The observed pattern rotation between the virtual cathode and YAG1 images, visible in the insets shown in Figure 1 results from the Larmor precession induced as the beam propagate through the L3 magnetic lens. The rotation angle is given by [12]: $\theta = \int_0^\infty [eB(r=0,z)]/[2m\gamma(z)\beta(z)c]dz$ where $B(r=0,z)$ is the axial component of magnetic field experienced by the beam, γ the beam's Lorentz factor and $\beta \equiv [1 - \gamma^{-2}]^{1/2}$. The rotation angle was numerically found to be $\theta = 55$ deg which compares well with the value of $\theta = 53 \pm 2$ deg for a peak axial magnetic field $\hat{B} = 0.339$ T.

PRELIMINARY ANALYSIS

To aid in understanding the experiment, we performed 3D PIC simulations of the beam dynamics using the program IMPACT-T. The code includes space charge force by solving Poisson's equation in the bunch's rest frame [13]. IMPACT-T was ran with a simplex optimizer to fine-tune the operating parameters of the accelerator used in the model to match the low charge measurements. The set of parameters obtained are compiled in Table 1 and are in good agreement with the settings inferred from the accelerator control system. The initial distributions used in our numerical simulations were generated with a quasi-random generator using the digitized pictures of the laser transverse density captured on the virtual cathode. As the total charge associated to the multibeam is

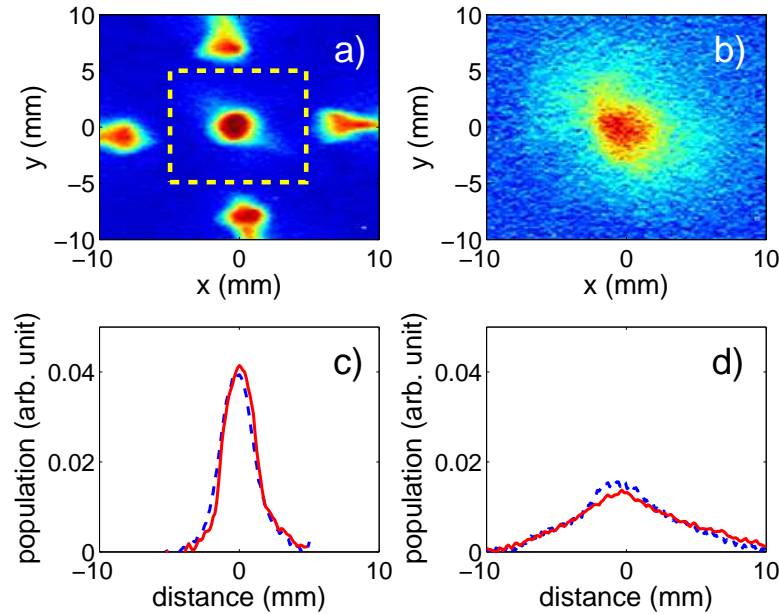


FIGURE 3. (Color) Two-dimensional transverse beam density and corresponding horizontal (blue line) and vertical (red dashed line) projections for the cases with [$Q = 0.93 \pm 0.05$ nC] (a,c) and without (b,d) [$Q = 0.17 \pm 0.03$ nC] surrounding beamlets.

increased to ~ 1 nC space charge become significant resulting in (1) a change in beamlet intra-dynamics and (2) in interactions between the beamlets. Such interactions result in the development of unexpected features that depend on the initial pattern [14]. In Figure 2 we present the measured and simulated transverse distributions at YAG1 location for different values of the magnetic fields \hat{B} . The simulations reproduce the main features experimentally observed especially the tail formations on the peripheral beamlets. For large values of the magnetic field the central beamlet appears confined. This space-charge-induced focusing effect is confirmed by masking the surrounding beamlets: the average central beamlet rms transverse beam size increases from 1.1 ± 0.3 mm to 3.9 ± 0.3 mm; see Figure 4. Numerical simulations performed for various solenoid settings indicate that the surrounding beamlet guide the central beamlets and thereby maintain the transverse emittance $\varepsilon_{\perp} \equiv [(\langle \beta_{\perp} \gamma \rangle^2 \langle x_{\perp}^2 \rangle - \langle x_{\perp} (\beta_{\perp} \gamma) \rangle^2]^{1/2}$ (where x_{\perp} and β_{\perp} are respectively the considered transverse coordinate and the corresponding velocity) for a longer distance. This is illustrated in Figure 4: the case of the central beamlet with surrounding beamlets is the only one that simultaneously contain the transverse beam size to a small size and maintain the transverse emittance almost constant downstream of the rf gun and solenoid (i.e. for $z > 0.5$ m).

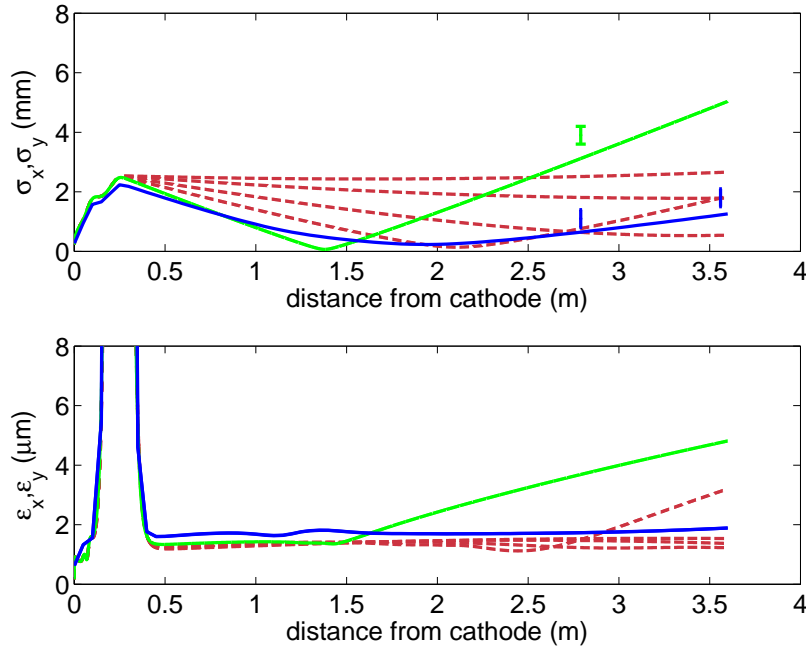


FIGURE 4. (Color) Transverse rms beam sizes (top) and corresponding emittance (bottom) evolution for the central beamlet along for different value of L3 peak axial magnetic field $\hat{B} \in [0.351, 0.375]$ T (dashed red lines). The cases shown in Figure 3 correspond to the solid blue (surrounding beamlets present) and green (central beamlet alone) lines. The corresponding data measured at YAG1 and YAG2 are also shown.

CONCLUSION & OUTLOOK

Although in the experiment discussed herein we used an external focusing element, a magnetic lens, to force the beamlets to cross each other and effectively result in the focusing of the central beamlet, it is generally possible, by a proper design, to avoid the use of such an external focusing element. Using other configurations for surrounding beamlets, e.g. a ring, could provide a mean for tailoring the bunch transverse distribution. The technique discussed here might have applications in high-brightness electron sources, e.g. based on superconducting rf-gun, where the use of an external field to focus/shape the beam is generally difficult.

ACKNOWLEDGMENTS

This work was supported by the US Department of Energy under Contract No. DE-FG02-04ER41323 with Northern Illinois University and by the US Department of Education under contract P116Z010035 with the Northern Illinois Accelerator and Detector Development. The work of P.P. is partially supported by the US Department of Energy under contract No. DE-AC02-07CH11359 with the Fermi Research Alliance, LLC.

REFERENCES

1. see for instance: LCLS Conceptual design report, report SLAC-R-593/UC-414, SLAC (2002); TESLA Technical design report Imprint No. DESY 2001-011 or ECFA 2001-209 (2001).
2. see the word wide website
<http://www.linearcollider.org>.
3. W. Gai, P. Schoessow, B. Cole, R. Konecny, J. Norem, J. Rosenzweig, and J. Simpson, *Phys. Rev. Lett.* **61**, 2765 (1988).
4. R. L. Gluckstern, *Phys. Rev. Lett.* **73**, 1247 (1994).
5. S. Bernal, R.A. Kishek, M. Reiser, "Observations and Simulations of Particle-Density Oscillations in an Apertured, Space-Charge Dominated Electron Beam", in *Proceedings of the 1985 IEEE Particle Accelerator Conference* (Vancouver, BC), 1791 (1985).
6. J.S. Fraser, R.L. Scheffield, E.R. Gray, and G.W. Rodenz, "High-Brightness Photoemitter Injector for Electron Accelerators", in *Proceedings of the 1985 IEEE Particle Accelerator Conference* (Vancouver, BC), 1791 (1985).
7. F. Zhou, I. Ben-Zvi, M. Babzien, X. Y. Chang, A. Doyuran, R. Malone, X. J. Wang and V. Yakimenko, *Phys. Rev. ST Accel. Beams* **5**, 094203 (2002).
8. C. Lejeune and J. Aubert, *Adv. Electron. Electron Phys. Suppl.* **A 13**, 159 (1980).
9. M. Reiser *et al.*, *Phys. Rev. Lett.* **61**, 2933 (1988).
10. I. Haber, *et al.*, *Phys. Rev. A.* **44**, 8 (1991).
11. information on the Argonne Wakefield Facility are available at the word wide website
<http://gate.hep.anl.gov/awa>.
12. M. Reiser *The Theory and design of Charged Particle Beams*, Wiley series in beam physics and accelerator technology, Edited by John Wiley & Sons, Inc. (1994).
13. J. Qiang, S. Lidia, R. D. Ryne and C. Limborg-Deprey, *Phys. Rev. ST Accel. Beams* **9**, 044204 (2006).
14. M. Rihaoui, W. Gai, P. Piot, J. Power, Z. Yusof, in preparation.